A ZVZCT Power Converter Topology for Variable Reluctance Machine Drives

Leví P.B. de Oliveira, Edison R. da Silva, Antônio M. N. Lima, Cursino B. Jacobina
Department of Electrical Engineering, Federal University of Paraiba
C.P. 10.105, Campina Grande, PB., 58.109-970 Brazil
Tel.: +55 (83) 310-1407, Fax: +55 (83) 310-1418, e-mail: edison@dee.ufpb.br

Abstract - **This proposed paper introduces a soft-switched version of the Miller's converter with the important characteristic of the converter switches operating simultaneously under zero voltage transition and zero current transition (ZVZCT). It is shown that its flexibility satisfies the requirements for implementation of different control strategies even though the converter has a lower number of switches when compared to the symmetric converter. Its ZVZCT characteristic is demonstrated by experimental results, which also confirm its flexibility for using different control techniques.**

I. INTRODUCTION

A number of converter topologies for Switched Reluctance Motors (SRM) drives have been proposed [1]-[4]. In SRM the operating conditions can be divided into low and medium speed region (constant torque, *T*, operation), high speed region (constant power, ωT, operation), and very high speed region (constant ωT^2 operation) [5]. Although the efficiency is a dominant criterion for an application over the entire operating region (e.g. traction), other drive performance, as for example the torque ripple, have a larger weight in some of the operating areas. Depending on the power level, the use of different control strategies for different regions of the torque-speed diagram can improve the overall performance of a SRM [5] Therefore, it is advantageous to have a flexible controller structure in which different control strategies can be implemented to optimize the drive performance. One of these structures is the Miller's converter [2].

On the other hand, a number of different soft switching techniques have been applied to SRM drives [6]-[8]. Among these, the soft-switched version of the DC-link version has a small number of components but suffer from high voltage stresses [8]. Instead, the voltage rating of the inverter components is limited to the source value in the soft-switched version of the symmetric converter introduced in [7]. However, such converter has a larger number of components when compared to other topologies [6][8].

This paper introduces a soft-switched version of the Miller's converter with the important characteristic of the converter switches operating simultaneously under zero voltage transition and zero current transition (ZVZCT). It is shown that its flexibility satisfies the requirements for implementation of different control strategies even though the converter has a lower number of switches when compared to the symmetric converter. Its ZVZCT characteristic is demonstrated by experimental results, which also confirm its flexibility for using different control techniques.

II. CONTROL STRATEGIES

It has been shown that for a low speed region of SRM, a low torque ripple is required, to prevent speed oscillations [10]. This performance can be achieved by an imposed profile of the phase current waveforms. Instead, when the speed increases the importance of a low torque ripple is reduced and the efficiency becomes the key criterion for the drive performance.

The three-phase Miller's converter scheme (Fig. 1) [2] is able to satisfy the requirements above by adequately choosing the modes to be used. Three basic modes of operation do exist for each phase (see Fig. 2). In *Mode I (powering mode)* switches S_a and S_f are on and $v_a = V_d$ (Fig. 2a); in *Mode II (recovery mode)* switches S_a and S_f are off, $v_a = -V_d$, the winding current decreasing through diodes D_a and D_f (Fig. 2b); in *Mode III (freewheeling mode)*, Fig. 2(c), S_a is on (off) and S_f is off (on) causing the current to freewheel through S_a (S_f) and D_f (D_a).

The torque produced by SRM depends on both the variation of the inductance in terms of rotor position and the current in each phase winding. The idealized motor inductance and different winding current profiles are presented in Fig. 3(a) and Fig. 3(b). The self-inductance varies accordingly to the rotational angle θ of the motor and the characteristic of all the phases are approximately the same except that they are shift one in relation to the others. The torque produced by SRM's depends on both the variation of the inductance in terms of rotor position and the current in each phase winding, that is,

$$T_{en} = \frac{1}{2}\frac{dL_n(\theta)}{d\theta} i_n^2 \qquad (1)$$

where subscript *n* represents one of subscripts *a*, or *b*, or *c*, *etc.* for winding currents and inductances.

Although the inductances can be measured experimentally at different rotor positions [9], they can be considered to vary linearly up and down between a maximum and a minimum value, as

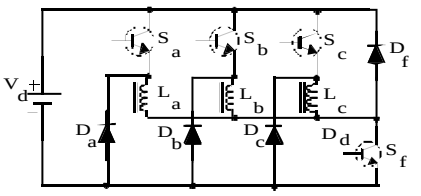

Fig. 1. Hard-switched version of a four-phase Miller's

schematically depicted in Fig. 4. From that figure,

$$\begin{aligned} L_a(\theta) &= L_{\min} && \text{for } \theta_1 \le \theta \le 0 \\ &= L_{\min} + \theta && \text{for } 0 \le \theta \le \beta_s \\ &= L_{\max} && \text{for } \beta_s \le \theta \le \beta_r \\ &= L_{\max} - K(\theta - \beta_r \beta_s) && \text{for } \beta_r \le \theta \le \beta_r + \beta_s \end{aligned} \qquad (2)$$

in which β_s and β_r are parameters of the SRM and $K = (L_{max}-L_{min})/\beta$ [10].

A. Individual Current Control

The waveform of current i_a is expanded in Figs. 4(a) to (f) to show different current profile possibilities in which three regions can be considered:

1) Increasing current (IC) region. Mode I ($v_a = V_d$) can be used to increase the winding current in this region until it reaches the top value, as in Figs. 4(d) to 4(f); an alternative [Fig. 4(c)] is to impose the current profile by alternating Mode I with either Mode II (*Strategy* V_d,*0*,V_d) or Mode III (*Strategy* V_d,-V_d,V_d), .

2) Top current (TC) region. The current in the TC region can be regulated by either Strategy V_d,-V_d,V_d [Figs. 4(c) and 4(d)] or Strategy V_d,*0*,V_d but, also, can just freewheel [*Strategy 0, as* in Fig. 4(e)]. Strategy *O* reduces switching losses in the TC region.

3) Decreasing current (DC) region. The current can be decreased with the application of either $v_a = -V_d$ or by imposing its shape, as in Fig. 4(c).

B. Current Control with Overlapping

During the transition between two phases, the torque ripple can be minimized by an approach named overlapping. With this purpose, the two phases conduct simultaneously over an extended predetermined period, one of them in the IC region and the other in the DC region. The simplest possibility is to apply a positive voltage to the incoming phase while either Mode II or Mode III is employed to reduce to zero the current in the outgoing phase. In this case, some aspects that influence the torque ripple should be observed. During overlapping the inductance of the incoming phase is low and the inductance of the outgoing phase is very large at this time. Therefore, if the positive voltage is employed the current increases fast. Also, when freewheeling is used to decrease the current in DC region this takes long time, which limits the high frequency operation. To overcome this problem two other possibilities are discussed next.

1) Technique I: The torque control strategy is based on following a contour for each of the phases of the SR motor such that the sum of torques produced by each phase is constant and equals

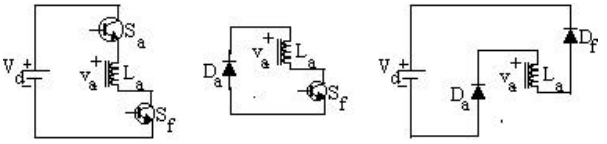

(a) Mode I (b) Mode II (c) Mode III

Fig. 2. Modes of operation for one leg

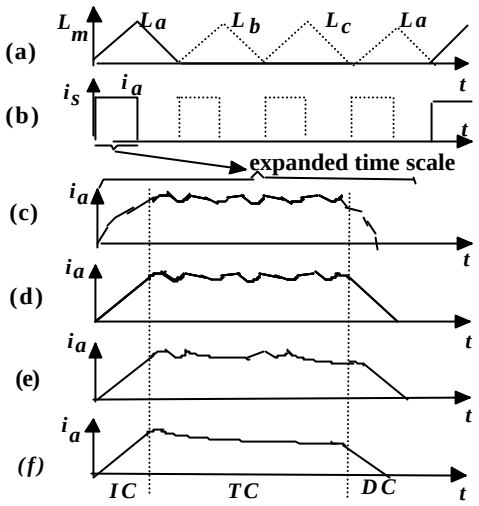

Fig. 3. Self-inductance and current profiles; strategies for current control.

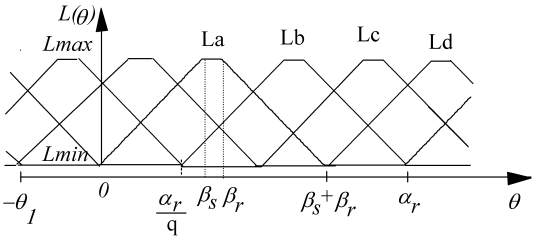

Fig. 4. Variable winding inductance in a SRM of 3 phases

the desired torque T_{ref}. With this purpose, a contour function $f_T(\theta)$ is defined such that

$$T_{total} = T_{ref} f_T(\theta) \qquad (3)$$

where $f_T(t)\sum_{k=1}^{n} f_k(\theta) = 1$with f_k being the contour function for the *k-th* phase. The contour function $f_T(\theta)$ can be a function of cosinus [9] or simply a cosinus. In this last case, the current references inside the overlapping interval, Δt, of transfer from phase *a* to phase *b* are

$$\begin{aligned} I_a^* &= \sqrt{\tfrac{1}{K}[1-\cos(t-t_o)]} \\ I_b^* &= \sqrt{\tfrac{1}{K}[1-\cos(t-t_o)]} \end{aligned} \quad . \qquad (4)$$

Considering the profile to be linear in that interval leads to simpler

current references

$$I_a^* = \sqrt{\frac{2}{K}(1-\frac{t-t_o}{\Delta t})}$$
$$I_b^* = \sqrt{\frac{2}{K\Delta t}(t-t_o)} \quad . \qquad (5)$$

2) Technique II: Phase A is kept in its discharging stage, while the increase of the current in phase B is controlled (rise control). The reference for the current in phase b is determined as a function of the actual current in phase a, that is,

$$I_b^* = \sqrt{I_a^* - i_a} \qquad (6)$$

III. THE PROPOSED SOFT-SWITCHED TOPOLOGY

Differently from the symmetric configuration proposed in [7], the proposed topology (Fig. 5) can operate with any number of phases having a smaller number of components. Capacitor C_{r2} and diodes from D_a to D_d allow main switches S_a, S_b, and S_c to operate under simultaneous zero voltage transition and zero current transition, ZVZCT. In particular, the connection of switch S_r - its sense is the opposite of that in [13] - makes possible to conceive an adequate switching sequence for the auxiliary circuit (marked by dashed lines) so that switch S_m also operates under ZVS/ZCS.

A. Operation Steps from Mode II to Mode I

An equivalent circuit of can be used to describe the sequential equivalent circuits for changing from Mode II to Mode I and vice versa. One cycle of operation is composed of eight stages (or sub-modes), as indicated from Fig. 6(a) to 6(i). When employed together with the modes in Section I, these stages allow current control and its transfer from one phase windings to another. They will be explained next with the help of the principal waveforms presented in Fig. 7.

1) Stage I (Freewheeling sub-mode, $t < t_1$): Suppose that initially the current in phase a, i_a, is freewheeling through switch S_{ab}, diode D_a, and winding L_a of phase a as shown in Fig. 6(a). In fact the current in phase a is decreasing but it will be considered as a constant equal to I_a during the commutation process. Suppose, also, that capacitor C_{r1} is charged with a voltage V_1, and C_{r2} is completely discharged. Switches S_m, S_r, and S_a are off during this interval.

2) Stage II (First resonant sub-mode, $t_1 < t < t_2$): In this stage, switches S_r, and S_a are turned on under ZCS and ZVS/ZCS, respectively. A resonant mode starts and the energy stored in capacitor C_{r1} is transferred to inductor L_r. This interval ends when the resonant current reaches the value I_a of the winding current i_a and diode D_a turns off. For an adequate operation in this interval it is necessary that

$$2V_d\sqrt{\frac{C_{r1}}{L_r}} > I_a \qquad (7)$$

so that the resonant current reaches the value I_a. At the end of the interval

$$v_{Cr1}(t_2) = V_2 = V_d - \sqrt{4V_d^2 - \frac{L_r}{C_{r1}}I_a^2} \qquad (8)$$

3) Stage III (Second resonant sub-mode, $t_2 < t < t_3$): After D_a blocks, a new resonant mode starts charging the capacitor C_{r2} with the help of the energy stored in L_r at the end of the previous interval [Fig. 6(d)]. When the voltage in capacitor C_{r2} reaches the value V_d, diode D_m turns on. For $C_{r1}/C_{r2} >> 1$ the condition to be observed can be shown to be

$$V_d - 2V_2 > \frac{I_a}{\sqrt{k_c}}(\frac{\pi}{2}-\phi)\sqrt{\frac{C_{r1}}{L_r}} \qquad (9)$$

where $\tan\phi = \frac{V_d - V_2}{I_a}\sqrt{(k_c+1)\frac{C_{r1}}{L_r}}$, $k_c = C_{r1}/C_{r2}$ a

$V_2 = V_d - \sqrt{4V_d^2 - \frac{L_r}{C_{r1}}I_a^2}$.

4) Stage IV (Third resonant sub-mode, $t_2 < t < t_3$): C_{r1} continues to charge resonantly until it reaches the value of the source voltage and D_0 starts conducting.

5) Stage V (Linear sub-mode, $t_4 < t < t_5$): During this interval, a current flows by either D_m or S_m. First, the excess of energy stored in the inductor is fed back to the source voltage V_d via the diode D_m. Next, D_m turns off and the current starts increasing in S_m while the current in L_a decreases. To guarantee ZCS/ZVS turns on for S_m a gate signal must be applied before D_m turn off.

6) Stage VI (Fourth resonant sub-mode, $t_5 < t < t_6$): After the current in S_m reaches the value I_a, a new oscillation starts, now through the path C_{r1}-L_r-D_a-S_m, and the capacitor voltage reverses completely.

7) Stage VII (Powering sub-mode, $t_6 < t < t_7$): In this stage, the converter is in the powering sub-mode until the control commands the turning off of S_m.

8) Stage VIII (Discharge of C_{r2}, $t_7 < t < t_8$): After S_m is turned off under ZVS, the current in winding a, I_a, discharges C_{r2} in a linear mode. When v_{Cr2} reaches zero, D_a starts conducting and this ends the operating cycle. From Stage VI it can be seen that $V_1 = -V_d$.

B. Operation Steps from Mode I to Mode III

When a change from Mode I to Mode II is required, S_m, S_a, and S_f must be turned off so that the winding current flows through diodes D_a and D_f. The process for turning off S_m and S_a is the same

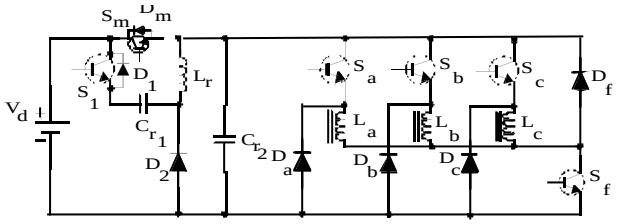

Fig. 5. Soft-switched version of a three-phase converter

as above.

C. Operation Steps from Mode III to Mode II

This change is achieved by turning S_f on.

D. Operation Steps for Overlapping

The modes of operation for overlapping between two phases are indicated in Fig. 8. For simplicity, they are presented in the HS version of the converter in Fig. 2. Overlapping can be controlled by using such modes.

VI. Simulated and Experimental Results

Simulated results have been performed for a three phase SRM drive in which the parameter values for the circuit are $V_d = 60$ *V*, $I_a =$ *2 A*, $C_{r2} = 1$ *nF*, $C_{r2} = 100$ *nF*, $L_r = 50$ *mH*. The SRM has a maximum inductance of *52 mH*,a minimum inductance of *8 mH* and a winding resistance of *2.2* **W.**Figure 9 shows the simulated results for the voltage v_{Cr1} and torque T_e and currents i_a and i_b, when Technique I is used with a ramp contour function during the overlapping interval, the current being regulated by Strategy V_d, 0,V_d. It should be noted that the maximum voltage across C_{r1} is limited by V_d. Adequate results are obtained with only the control of the current rise (Technique II) with the same strategy, as shown in Fig. 10. Results at high speed when the torque ripple becomes less important are not presented in this text.

The three phase converter in Fig. 6 has been implemented experimentally to verify the principles of soft-switching in the converter and the control principles studied. the tree-phase SRM H55BMBJL, 12 stator poles, rated current of *2.5 A, 120 V DC.* Except for a maximum inductance of and a winding resistance of *1.5* **W,**all other parameters are the same as for the simulated results. Fig. 11 shows the experimental results for 477 rpm corresponding to the simulated cases of overlapping with (1) cosinus control amd (2) linear control of both currents, and (3) rise control of the increasing current. Note that the torque ripple is smaller in the case of rise control. Advancing the firing angle, as done for the simulated results, would reduce the experimental torque ripple. The existing difference in the capacitors voltage waveforms are mainly due to non stored pulses in simulation. Finally, Fig. 12 compares the voltage across S_a and S_m with their corresponding currents. It can be observed that voltage is zero while the current decreases during turn-off and that

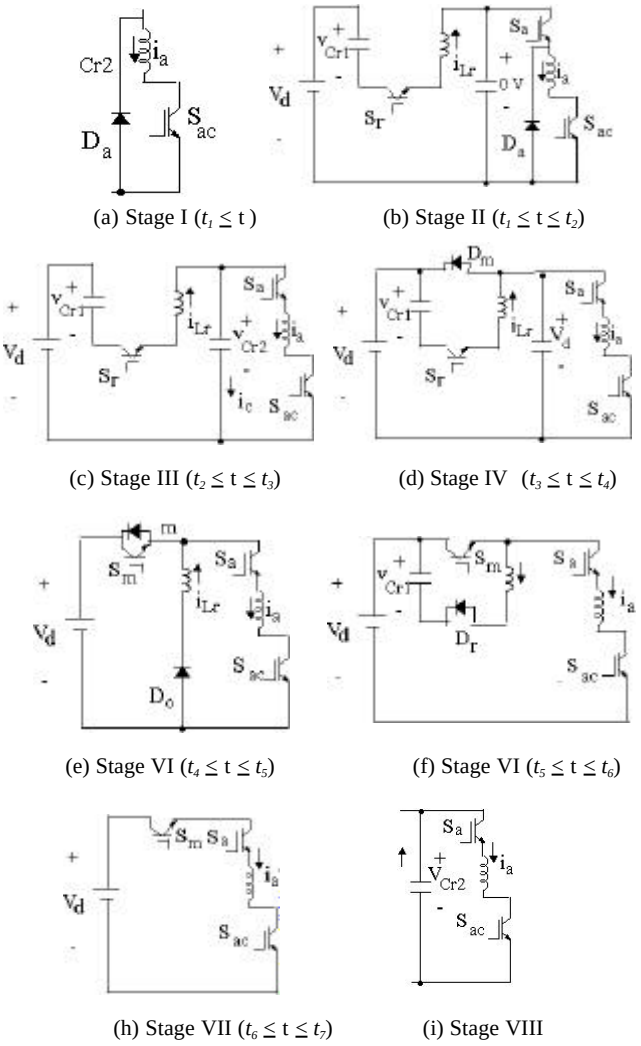

(a) Stage I ($t_1 \le t$) (b) Stage II ($t_1 \le t \le t_2$)

(c) Stage III ($t_2 \le t \le t_3$) (d) Stage IV ($t_3 \le t \le t_4$)

(e) Stage VI ($t_4 \le t \le t_5$) (f) Stage VI ($t_5 \le t \le t_6$)

(h) Stage VII ($t_6 \le t \le t_7$) (i) Stage VIII

Fig. 6. Equivalent circuits for one cycle of operation.

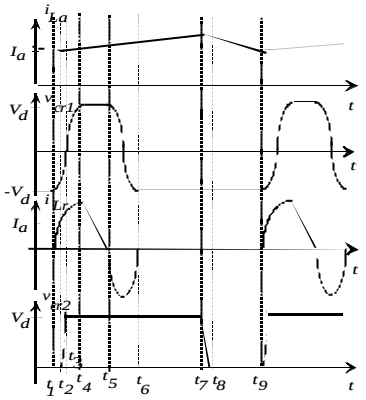

Fig. 7. Principal waveforms for the circuit in Fig. 5(a)

the voltage remains near zero when the switch is turned on. These results confirm ZVZCT condition of the proposed circuit and its flexibility as well.

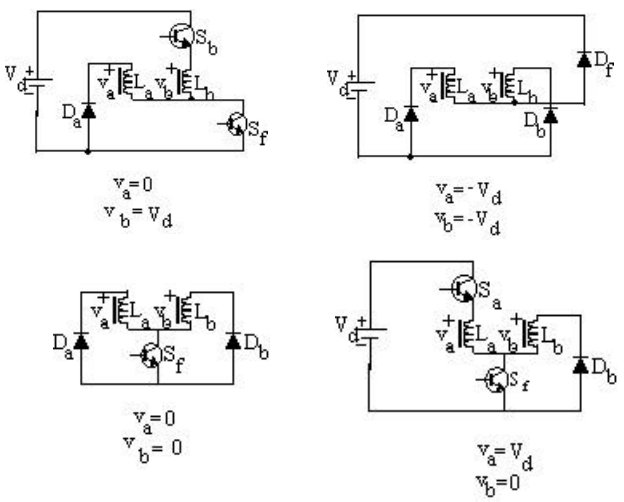

Fig. 8. Modes for overlapping between two phases.

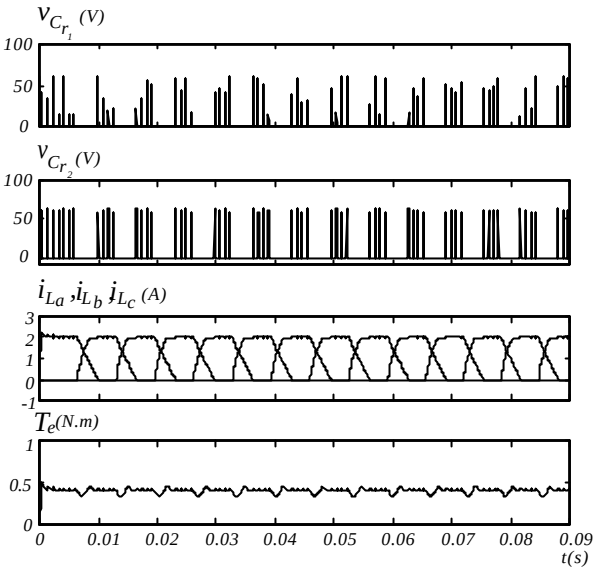

Fig. 9. Simulated results: Technique I with ramp control

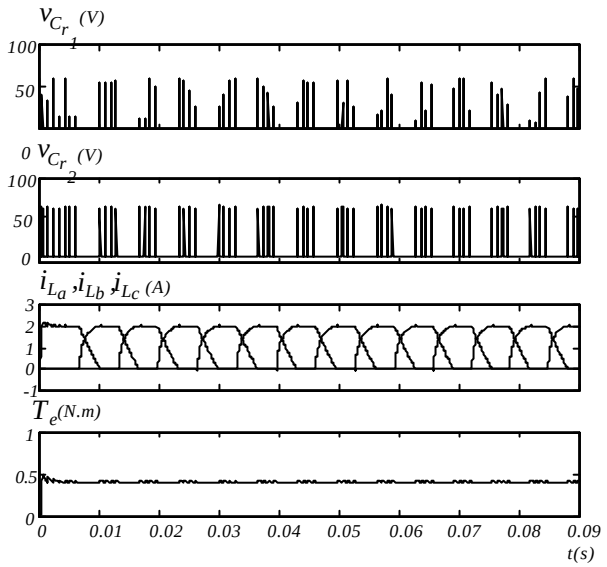

Fig. 10. Simulated Results: Technique II (rise control)

CONCLUSION

This paper presented a soft-switched version of the Miller's converter as applied to a three-phase SRM. The converter, which operates under ZVZCT condition, has shown to allow the application of different control techniques useful to optimize the drive performance. During the overlap interval, in which the current is transferred from one phase to another, a strategy in which it is controlled the shape of the current in only one of the phases has presented the best results in terms of torque ripple. Experimental results confirmed both the ZVZCT characteristic of the converter and its flexibility for using different control techniques.

ACKNOWLEDGMENTS

The authors wish to thank Emerson Motors for providing the motor used in the experimental tests.

REFERENCES

[1] A. Hava, V. Blasko, and T.A. Lipo, "A modified C-dump converter for switched reluctance machines", IEEE IAS'91 Conference Record, 1991, pp. 886-891.

[2] S. Vukosavic and V. Stefanovic, "SRM inverter topologies: a comparative evaluation", *IEEE Trans. on Ind. Appl.*, Vol. 27, No. 6, Nov./Dec. 1991, pp. 1034-1047.

[3] M. Ehsani, J.T. Bass, T.J.E. Miller, and R.L. Steigerwald, "Development of a unipolar converter for switched reluctance motor drives", *IEEE Trans on Ind. Appl.*, vol. IA-23, No. 3, 1987, pp. 545-553.

[4] S. Mir, I. Hussein, amd M.E. Elbuluk, "Energy-efficient C-dump converters for switched reluctance motors", *IEEE Trans on Power Electronics*, vol. 12, No. 12, Sept. 1997, pp. 912-921.

[5] J. Reinert, R. Inderka, M. Menne, and R.W. De Doncker, "Optimizing performance in switched reluctance drives", IEEE APEC'98 Conference Record, 1998, pp. 765-770.

[6] S.S. Park and T.A. Lipo, "New series resonant converter for variable reluctance motor drive", Research Report 92-9, WEMPEC, University of Wisconsin-Madison, March 1992.

[7] G.H. Rim, W.H. Kim, and J.G. Cho, "ZVT Single Pulse-Current Converter for Switched Reluctance Motor Drives", IEEE APEC'96 Conference Record, 1996, pp. 949-955.

[8] E.R. da Silva, L.P.B. de Oliveira, C.B. Jacobina, and A.M.N. Lima, "New soft-switched power converter topologies for variable reluctance machine drives", IEEE PESC'99 Conference Record, pp. 826-831.

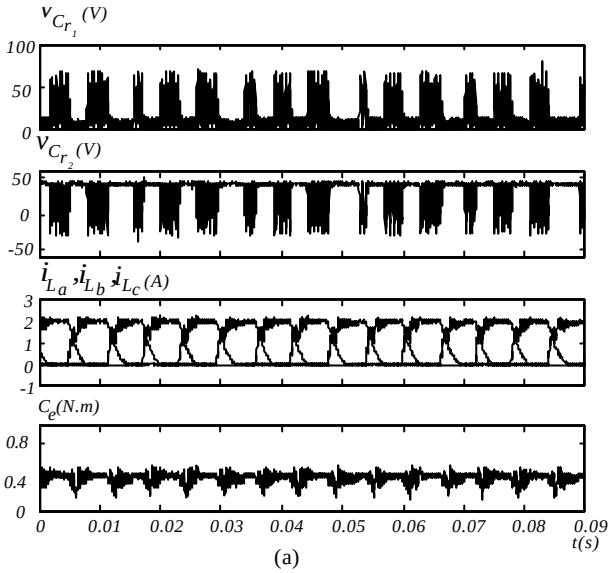

(a)

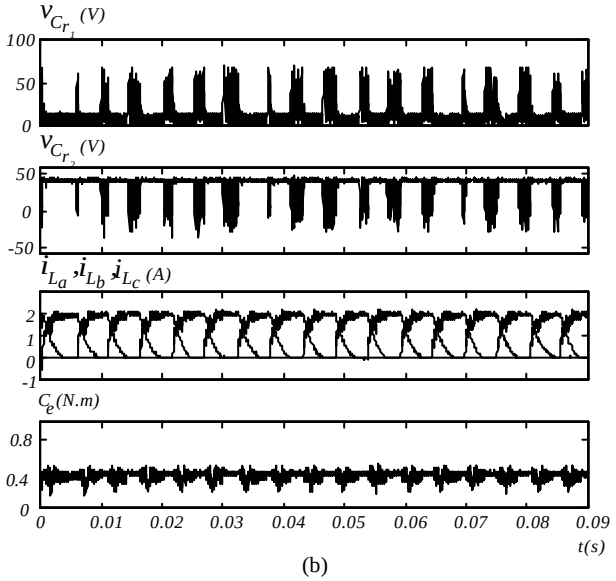

(b)

Fig. 11(cont.)

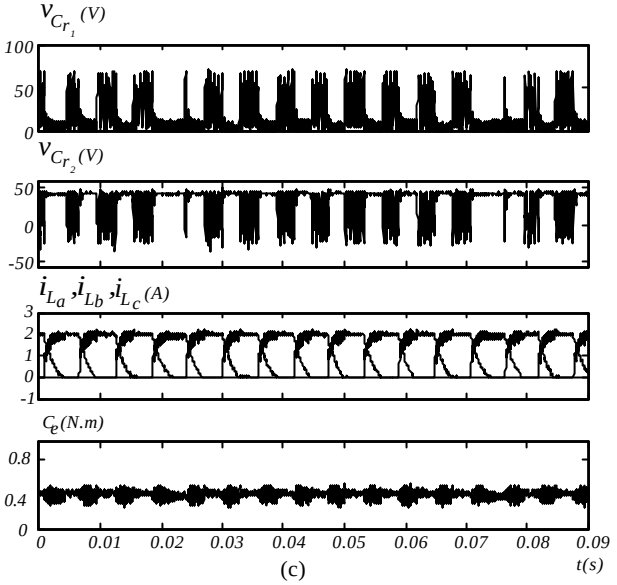

(c)

Fig. 11. Experimental results with use of $V_d, 0, V_d$ for regulating the top current. During the overlapping: (a) Technique I with cosinus control;

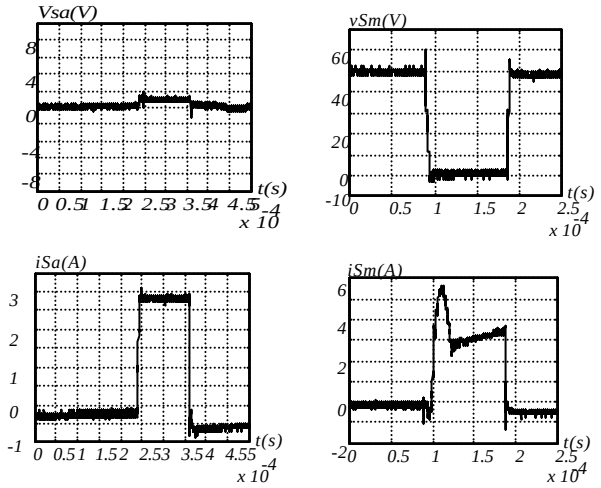

Fig. 12. Experimental results: verification of soft switching in switches S_a (left) and S_m (right),

[9] I. Hussain and M. Ehsani, "Torque ripple minimization in switched reluctance motor drives by PWM current control", *IEEE Trans. on Power Electronics*, Vol. II, No. 1, Jan. 1986, pp. 83-88.

[10] M.I. Valla and G. S. Buja, "Control characteristics of the SRM drives - part I: operation in the linear region", IEEE Trans. on Ind. Electron., Vol. 38, N. 5, 1991, pp. 313-321.